JOURNAL OF GEOPHYSICAL RESEARCH, VOL. 97, NO. D9, PAGES 10,069–10,081, JUNE 20, 1992

On the Transient Response of a Simple Coupled Climate System

KWANG-YUL KIM

Applied Research Corporation, College Station, Texas

GERALD R. NORTH AND JIANPING HUANG[1]

Climate System Research Program, Department of Meteorology, Texas A&M University, College Station, Texas

This paper presents quasi-analytical solutions to a class of coupled atmosphere-ocean models for time-dependent ramp- and step-forced climate changes. The model consists of a conventional two-dimensional energy balance model of the atmosphere with an oceanic mixed layer coupled to a deep ocean having vertical heat transports due to horizontally uniform vertical diffusion and upwelling. The solution is partitioned into the particular or asymptotic part and the homogeneous or transient part. This partitioning facilitates understanding the different time constants involved in the problem. For ramp forcing there are two time constants: the lag time in the asymptotic straight line warming solution and the characteristic adjustment time to the asymptotic curve. The lag behind the "no inertia" warming is a few decades, while the adjustment time to the asymptotic curve is several hundred years due to the restructuring of the thermal profile near the main thermocline. This is in strong contrast to the step-forcing scenario where the adjustment time to the new constant steady state is only a few decades. The latter experiment suggests that step-forcing scenarios are not very similar to ramp-forcing scenarios. The model produces a warming of $\sim 0.5°C$ over the last hundred years provided the simulation is started 200 years ago. An interesting feature of the solutions is that the land surface areas lead the ocean surface areas in heating up by $O(0.1°C)$. This may lead eventually to a fairly robust signature of the greenhouse forcing. Future models of this type probably need more horizontal dependence on the vertical heat transport parameters as well as horizontal transport mechanisms.

1. INTRODUCTION

Long records of global temperatures suggest that the global mean surface air temperature of the Earth has increased by about 0.5°C during 1880–1980 [e.g., *Jones et al.*, 1986; *Hansen and Lebedeff*, 1987]. The record clearly shows an irregular but steady increase of the global temperature. It has been speculated that this rise in the global temperature is due to the increased concentration of the greenhouse gases. At least the argument that the observed warming trend is above the natural variability of the climate system is very appealing [*Wigley and Raper*, 1990].

It has long been recognized that the transient response of the climate system depends strongly on the effective thermal inertia of the ocean. On the other hand, processes transporting heat from the surface to the deep ocean determine the effective heat capacity of the ocean. Therefore, earlier attempts to understand and to reproduce the signatures of the greenhouse gas warming via climate models with mixed-layer ocean were inadequate from the outset. These thin-slab ocean models tend to overestimate the global temperature increase during the early years because the thermal equilibrium is quickly reached in the absence of energy transport from the surface into the deep ocean.

Some preliminary basis for understanding the time-dependent response to greenhouse gas forcing has been established via climate models which include the deep ocean [e.g., *Hoffert et al.*, 1980; *Thompson and Schneider*, 1982; *Hoffert and Flannery*, 1985; *Schlesinger et al.*, 1985; *Schlesinger*, 1989; *Washington and Meehl*, 1989; *Wigley and Raper*, 1990; *Morantine and Watts*, 1990; *Manabe et al.*, 1990; *Schlesinger and Jiang*, 1990]. The prescription of the ocean is different from model to model. Some more detailed models have oceans forced by dynamically computed winds, currents, convective processes, etc. Some only have a schematic deep ocean with processes transporting heat from the surface to the depth, which increases the effective thermal inertia of the ocean. As suggested by *Hoffert and Flannery* [1985], vertical heat diffusion and upwelling may be two important processes essential to modeling the transient response.

One interesting class of studies considers the transient response of the globally averaged world [*Wigley and Raper*, 1990; *Morantine and Watts*, 1990] or zonally averaged world [*Watts and Morantine*, 1990; *Schlesinger and Jiang*, 1991] with a deep upwelling-diffusion ocean. Use of these simple mechanisms has illustrated the possible role of the deep ocean in the transient response of the Earth. These highly averaged models, however, have provided little insight into the geographical distribution of the warming signature, which is important in the study of impacts and in the issue of detection or attribution of the causes of climate change.

Another class of studies considers the CO_2 doubling response of general circulation models (GCMs) coupled with ocean general circulation models (OGCMs) to an abrupt increase in atmospheric CO_2. These formulations are presumably a more realistic representation of the Earth's climate system [*Schlesinger et al.*, 1985; *Washington and Meehl*, 1989; *Schlesinger and Jiang*, 1990; *Manabe et al.*, 1990]. Such studies in principle can provide important geographical and seasonal signatures of the greenhouse gas warming.

[1] On leave from Peking University, Beijing.

Paper number 92JD00581.
0148-0227/92/92JD-00581$05.00

Since simulations of large ensembles are prohibitively expensive for these models, however, results raise questions of sampling error bias. Because the oceanic processes have very long (and unknown) time constants, proper statistics could only be derived from ensembles of very long runs. Further, these comprehensive models may not have yet been properly tuned. Finally, as addressed by *Thompson and Schneider* [1982], the time-dependent response to gradual changes in forcing of the system may be quite different from the response to abrupt CO_2 doubling in several respects. *Washington and Meehl* [1989] report some such differences.

Considering the difficulties addressed above, it is desirable to develop approaches simpler than the coupled GCMs yet detailed enough to simulate a meaningful transient response particularly of the surface temperature field. One such candidate is a three-dimensional simple energy balance model (EBM). In this paper we treat the ocean as a mixed-layer thin slab atop a deep ocean which has horizontally uniform vertical heat diffusion and a large-scale constant upwelling. The vertical diffusion and upwelling processes transport the incoming energy imbalances downward thereby thermally connecting the warmer mixed layer with the deep ocean. Also in recognition of the differential role of the land and the ocean, the model has an explicit two-dimensional geography. Simple energy balance models of the surface temperature field have been successful in reproducing the large-scale features of the Earth's climate in a number of studies [*North et al.*, 1983*a*, 1992; *Hyde et al.*, 1989, 1990; *Leung and North*, 1992; *Kim and North*, 1991]. In particular, the models seem particularly adept at simulating geographical distributions of the seasonal cycle and the continuum fluctuations with time scales between 2 months and 5 years. While more accurate GCMs should eventually be used routinely in the simulations of the transient response of large-scale climate, EBMs are expected to provide valuable insights and baseline solutions for comparison.

In this paper we provide solutions to two time-dependent scenarios of forced climate change, the response to an abrupt change in CO_2 and the response to an exponentially increasing concentration of CO_2. It is known that an increase in CO_2 leads to a decrease in the outgoing radiation at the top of the atmosphere for a given surface temperature. Furthermore, the dependency is logarithmic [e.g., *Wigley*, 1987; *Shine et al.*, 1990]. Hence, an exponentially increasing load of CO_2 leads to a linearly decreasing amount of outgoing radiation for a given surface temperature. This allows us to model the radiation imbalance as a linear ramp function switched on at $t = 0$, say $A(t) = A_0 - \gamma t$. The value of γ depends on the doubling rate of CO_2; e.g., $\gamma = 0.06$ W m^{-2} yr^{-1} for the case of doubling every 70 years (1% per year). This value might be appropriate for modeling the future. A value half as large might be more realistic in modeling the last 100 years.

Additional insight is gained through partitioning the solutions to the linear response into the "particular" solution and the "homogeneous" or "transient" solution, the latter being the decaying portion of the solution dependent on the initial conditions. To illustrate this process, consider a very simple slab model of climate which has a uniform heat capacity per unit area C over the globe; C is nominally proportional to the thickness of the slab. The energy balance may be written

$$C\frac{dT}{dt} + BT = \gamma t H(t), \tag{1}$$

where $T(t)$ is the excess of globally averaged temperatu over the equilibrium steady state value before the ramp for ing is turned on, B is a radiative damping coefficient, and γt represents a linearly increasing imbalance of the externally imposed heating (e.g., an exponentially increasing concentration of CO_2). The factor $H(t)$ is the Heaviside step function, 0 for $t < 0$, 1 for $t \geq 0$, which indicates that the forcing is switched on at $t = 0$. A particular solution for $t > 0$ is

$$T_p(t) = \frac{\gamma}{B}(t - \tau_0), \tag{2}$$

where $\tau_0 \equiv C/B$ is the "lag" behind the value that would be obtained in the absence of any thermal inertia. The appropriate homogeneous solution to go with this particular solution is

$$T_h(t) = (T_0 + \frac{\gamma}{B}\tau_0)e^{-t/\tau_0}. \tag{3}$$

The transient solution depends explicitly on the initial condition T_0. It decays with the same characteristic time $\tau_0 = C/B$ as the lag occurring in the particular or asymptotic solution. Note that the second term in parentheses above cancels the lag in the particular solution when $t = 0$. Therefore, the complete solution

$$T(t) = T_p(t) + T_h(t) \tag{4}$$

yields $T(t = 0) = T_0$. The decomposition above gives us some idea of how the solution behaves. The asymptotic solution is approached as the initial condition decays away. In addition there is another large term which must decay away, namely, the "lag compensator," the second term (3). These points are illustrated in Figure 1*a*. In this paper we use the same partitioning to study the adjustments of a deep diffusive-upwelling ocean coupled to the surface energy balance model. As a second example, consider the case of step forcing: $\Delta A\, H(t)$ on the right-hand side of (1). In this case the particular solution is

$$T_p^{\text{step}}(t) = \frac{\Delta A}{B}, \qquad t > 0, \tag{5}$$

while the homogeneous solution has the same exponential decay form as (2):

$$T_h^{\text{step}}(t) = (T_0 - \frac{\Delta A}{B})e^{-t/\tau_0}. \tag{6}$$

Hence, in both cases the adjustment to the asymptotic form is accomplished in a time of the order of τ_0. The response to step forcing is illustrated in Figure 1*b*. In both Figures 1*a* and 1*b*, a somewhat arbitrarily chosen lag of 60 years was used for all the characteristic times: asymptotic lag, exponential adjustment time to the ramp forcing, and exponential adjustment time to the step forcing. We will find that in the deep diffusive-upwelling ocean coupled to the surface energy balance model these three adjustment times are not equal but quite different from each other, in some cases by an order of magnitude. Hence, it will prove to be misleading to use the step experiment to estimate the adjustment time for other forcing scenarios such as ramp-forcing cases.

In the next section we will describe an energy balance climate model with two-dimensional geography coupled wi the deep diffusive-upwelling ocean. Then we will derive essentially analytical solutions of the model to a class of time-dependent forcings utilizing the Laplace transforma-

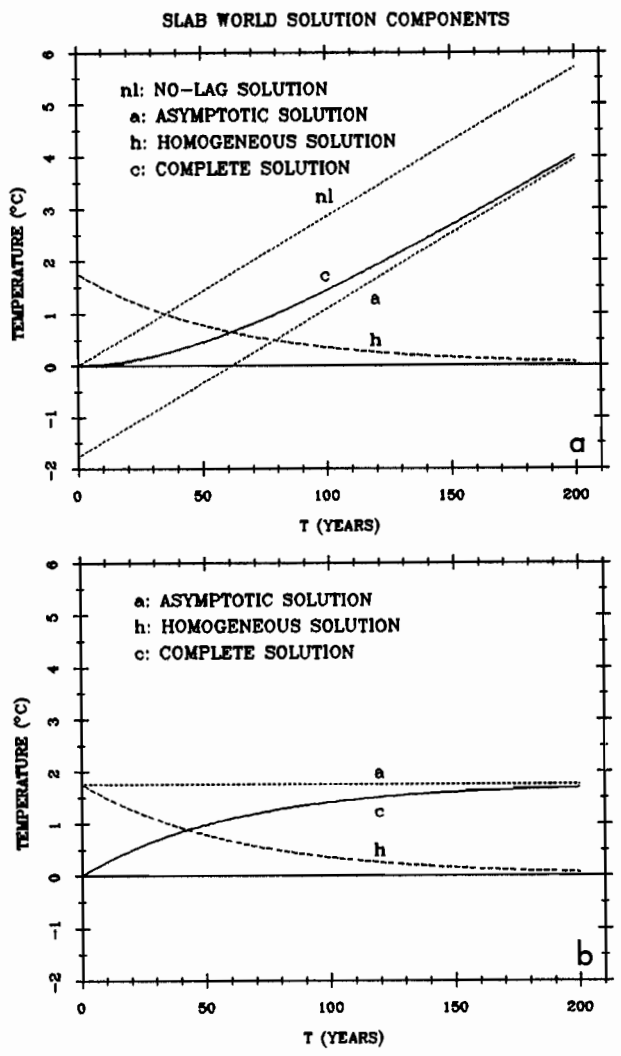

Fig. 1. Time-dependent solution components for the slab world described by equation (1). (*a*) Solutions for ramp forcing: nl is the solutions that would be obtained in the absence of any thermal inertia (the no-lag solution); a is the asymptotic or particular solution; h is the transient or homogeneous solution; c is the complete solution $T_h + T_p$. (*b*) Solutions for step forcing: a is the asymptotic or particular solution; h is the transient or homogeneous solution; c is the complete solution $T_h + T_p$. In all cases we have (arbitrarily) taken $\tau_0 \equiv C/B = 60$ years.

tion. Use of this technique results in significant computational savings. Finally, model results will be analyzed and applied toward the understanding of the transient response and warming signatures due to greenhouse gases.

2. MODEL

We next introduce our linear surface energy balance climate model coupled with a deep ocean with horizontally uniform vertical heat diffusion and a constant upwelling. Let $T(\hat{\mathbf{r}}, z, t)$ be the local departure of the temperature from its value at constant steady state, where $\hat{\mathbf{r}} \equiv (\theta, \phi)$ is a unit vector denoting a ray pointing out of the spherical surface at latitude θ and longitude ϕ, and z is depth (over ocean) below the mixed layer ($z \leq 0$). The heat equations in the oceanic interior and in the mixed layer slab are

$$\frac{\partial T}{\partial t} + w\frac{\partial T}{\partial z} = k\frac{\partial^2 T}{\partial z^2}, \qquad z \leq 0, \tag{7a}$$

$$C(\hat{\mathbf{r}})\frac{\partial T}{\partial t} + BT - \nabla \cdot \left(D(x)\nabla T\right) - wC^*(\hat{\mathbf{r}})T + kC^*(\hat{\mathbf{r}})\frac{\partial T}{\partial z} = F(\hat{\mathbf{r}}, t), \qquad z = 0, \tag{7b}$$

$$T \to 0 \quad \text{as} \quad z \to -\infty, \tag{7c}$$

$$T(\hat{\mathbf{r}}, z, t = 0) = T_0(\hat{\mathbf{r}}, z), \tag{7d}$$

where $x = \sin\theta$ is the sine of latitude, $C(\hat{\mathbf{r}})$ is the local heat capacity per unit area (C_W over the mixed-layer ocean, C_L over the land, and C_I over the permanent sea ice), $D(x) = D_0(1 + D_2x^2 + D_4x^4)$ is the local horizontal diffusion constant in the atmosphere and the mixed layer, $T(\hat{\mathbf{r}}, z, t)$ is the temperature field, $F(\hat{\mathbf{r}}, t)$ is the radiative forcing, B is slope of the best linear fit for the infrared emission to space, w is the upwelling speed, k is the vertical heat diffusion coefficient, and $C^*(\hat{\mathbf{r}})$ is the heat capacity of sea water per unit volume. Table 1 shows the values used in this study for these parameters.

Equation (7*a*) is the heat budget equation for the ocean interior, which originally was proposed to describe the maintenance of the main thermocline [e.g., *Munk*, 1966; *Overstreet and Rattray*, 1969; *Turner*, 1981]. Recently, renewed interest in (7*a*) has focussed on the role of the deep ocean in the transient response of the Earth's climate [*Hoffert et al.*, 1980; *Lebedeff*, 1988; *Watts and Morantine*, 1990; *Wigley and Raper*, 1990; *Morantine and Watts*, 1990]. In simulating the transient response of the Earth's climate, consideration of the effective thermal inertia of the deep ocean is essential. The upwelling and the vertical diffusion processes are regarded as important mechanisms which effectively remove heat energy from the mixed layer into the deep ocean, thereby increasing the effective heat capacity of the ocean far beyond that of the mixed-layer ocean. Note that in our formulation we impose the boundary condition that the thermal departure from initial equilibrium be zero

TABLE 1. Model Parameters

Symbol	Value	Reference
B	2.094 W m^{-2} °C^{-1}	*North et al.* [1983a]
C_W/B	4.6 years	*North et al.* [1983a]
C_I	$C_W/6.5$	*North et al.* [1983a]
C_L	$C_W/60$	*North et al.* [1983a]
C^*	$C_W/75$ m over ocean; 0 over land	present study
D_0/B	0.39 m^2	*North et al.* [1983a]
D_2	−1.33	*North et al.* [1983a]
D_4	0.67	*North et al.* [1983a]
k	varied $\in$ [2000,8000] m^2 yr^{-1}	present study
w	varied $\in$ [2,8] m yr^{-1}	present study

at infinite depth. We think of this deep temperature (actually, potential temperature) as being at freezing. Some authors have allowed this lower boundary condition to depend on some surface property such as the polar temperature where most deep water is presumably formed [*Hoffert and Flannery*, 1985]. We keep our formulation of the lower boundary condition fixed, maintaining the overall linearity of the system, and at the same time we avoid introducing another phenomenological parameter. However, we must keep in mind that this is an important constraint on our present approach.

Equation (7*b*) is the energy balance equation for the surface of the Earth including the mixed-layer ocean with time- and position-dependent radiative forcing $F(\hat{\mathbf{r}}, t)$. The surface is coupled with the deep ocean through the thermal forcing term at the bottom of the mixed layer:

$$F_{\text{bottom}} = wC^*(\hat{\mathbf{r}})T - kC^*(\hat{\mathbf{r}})\frac{\partial T}{\partial z}. \tag{8}$$

Other than this additional forcing term, (7*b*) is very much the same as its predecessors [e.g., *North et al.*, 1983*a*; *Hyde et al.*, 1990]. This surface energy balance model satisfactorily reproduces the geographical distribution of the annual and semiannual harmonics of the seasonal cycle of the Earth's climate mainly through the position-dependent heat capacity $C(\hat{\mathbf{r}})$. Recently, the model has also been shown to reproduce the geographical distribution of variance and other second-moment statistics when forced by simple noise forcing white in space and time [*Kim and North*, 1991; *North et al.*, 1992; *Leung and North*, 1992].

Equation (7) is difficult to solve in its present form for general initial condition field, $T_0(\hat{\mathbf{r}}, z)$, even for a fairly simple forcing $F(\hat{\mathbf{r}}, t)$. To facilitate finding the solution, we divide (7) into two parts as was done in the slab ocean example given earlier:

$$\frac{\partial T_p(\hat{\mathbf{r}}, z, t)}{\partial t} + w\frac{\partial T_p}{\partial z} = k\frac{\partial^2 T_p}{\partial z^2}, \qquad z \le 0, \tag{9a}$$

$$C(\hat{\mathbf{r}})\frac{\partial T_p}{\partial t} + BT_p - \nabla\cdot\left(D(x)\nabla T_p\right) - wC^*(\hat{\mathbf{r}})T_p + kC^*(\hat{\mathbf{r}})\frac{\partial T_p}{\partial z} = F(\hat{\mathbf{r}}, t), \qquad z = 0, \tag{9b}$$

$$T_p \to 0 \quad \text{as} \quad z \to -\infty, \tag{9c}$$

$$T_p(\hat{\mathbf{r}}, z, t = 0) = T_{p0}(\hat{\mathbf{r}}, z), \tag{9d}$$

and

$$\frac{\partial T_h(\hat{\mathbf{r}}, z, t)}{\partial t} + w\frac{\partial T_h}{\partial z} = k\frac{\partial^2 T_h}{\partial z^2}, \qquad z \le 0, \tag{10a}$$

$$C(\hat{\mathbf{r}})\frac{\partial T_h}{\partial t} + BT_h - \nabla\cdot\left(D(x)\nabla T_h\right) - wC^*(\hat{\mathbf{r}})T_h + kC^*(\hat{\mathbf{r}})\frac{\partial T_h}{\partial z} = 0, \qquad z = 0, \tag{10b}$$

$$T_h \to 0 \quad \text{as} \quad z \to -\infty, \tag{10c}$$

$$T_h(\hat{\mathbf{r}}, z, t = 0) = T_0(\hat{\mathbf{r}}, z) - T_{p0}(\hat{\mathbf{r}}, z). \tag{10d}$$

We will refer to the (unknown) dependent variable fields in (9) and (10) as the particular and the homogeneous solutions of (7). Note that the solution of (7) is the sum of the particular solution and the homogeneous solution. In the next section we will derive the particular solutions of (9) in closed form for the two special cases of forcing. We will also derive a semi-closed form of the homogeneous solutions for a useful special class of initial conditions.

3. Analytical Solutions

The particular solution is very easy to find in both the step- and ramp-forcing cases. Hence, we begin by solving for these in simple closed form. Then the transient solutions will be presented with details of the solution technique in the appendix.

Particular Solutions

Consider first the step function increase in CO_2. In terms of the radiative forcing,

$$F(\hat{\mathbf{r}}, t) = -\Delta A\, H(t), \tag{11}$$

where for a doubling, $\Delta A \approx -4.20$ W m^{-2}. It can easily be shown by insertion that the solution of (9) is

$$T_p = \alpha e^{\delta z}, \tag{12}$$

where

$$\delta = w/k, \tag{13}$$

$$\alpha = -\Delta A/B. \tag{14}$$

The particular or asymptotic solution to the instantaneous CO_2 doubling is the spatially uniform surface temperature rise which decays exponentially with depth. This result is consistent with *North et al.* [1983*b*].

Now consider the case of ramp forcing, $F(\hat{\mathbf{r}}, t) = \gamma t H(t)$. Let us try a solution of (9) in the form

$$T_p = \alpha(t - \tau(\hat{\mathbf{r}}) + z/w)e^{\delta z}. \tag{15}$$

Note that $\tau(\hat{\mathbf{r}})e^{\delta z}$ and $-(z/w)e^{\delta z}$ serve as local tempo lags of the response to the radiative forcing and that t latter vanishes near the surface in particular. It follows from (9*a*) that

$$\delta = w/k. \tag{16}$$

Furthermore, from the boundary condition (9*b*), it can be shown that

$$\alpha = \gamma/B, \tag{17}$$

$$B\tau(\hat{\mathbf{r}}) - \nabla\cdot\left(D(x)\nabla\tau(\hat{\mathbf{r}})\right) = C(\hat{\mathbf{r}}) + C^*(\hat{\mathbf{r}})/\delta, \tag{18}$$

where $\tau(\hat{\mathbf{r}})$ is the position dependent temporal lag of the particular solution. Noting that $1/\delta$ is the depth of the permanent thermocline, we shall refer to the right-hand side of (18) as the effective heat capacity. It is the total heat capacity per unit area of the water column down to the permanent thermocline including the mixed layer. The system (18) is a familiar damped diffusion process that can be solved for by well-known methods. It is the same equation that needs to be solved in the case of steady state EBMs, for example. It is easy to see that large effective heat capacity on the right-hand side leads to long delay times $\tau(\hat{\mathbf{r}})$ with diffusion serving to smooth the field. For later use, let us define

$$T_{p0} = -\alpha(\tau(\hat{\mathbf{r}}) - z/w)e^{\delta z}. \tag{19}$$

Before proceeding, we note that the solution has the shape of an instantaneously forced response, but with a lag that depends on horizontal and vertical location.

Transient Solutions

The homogeneous or transient solution which depends on the initial condition field is much more complicated to de-

rive. In this section we present the general path but relegate details to the appendix. To approach the problem, it is useful to eliminate the time by the use of the Laplace transformation [e.g., *Watts and Morantine*, 1990]. Equation (10) then is rewritten as

$$k\frac{\partial^2 \tilde{T}_h}{\partial z^2} - w\frac{\partial \tilde{T}_h}{\partial z} - s\tilde{T}_h = -T_{h0}, \qquad z \le 0, \tag{20a}$$

$$\left[sC(\hat{\mathbf{r}}) + B - \nabla\cdot\left(D(x)\nabla\right) - wC^*(\hat{\mathbf{r}}) + kC^*(\hat{\mathbf{r}})\frac{\partial}{\partial z}\right]\tilde{T}_h = C(\hat{\mathbf{r}})T_{h0}, \qquad z = 0, \tag{20b}$$

$$\tilde{T}_h \to 0 \quad \text{as} \quad z \to -\infty, \tag{20c}$$

$$T_{h0}(\hat{\mathbf{r}}, z) = T_h(\hat{\mathbf{r}}, z, t = 0) = T_0(\hat{\mathbf{r}}, z) - T_{p0}(\hat{\mathbf{r}}, z), \tag{20d}$$

where

$$\tilde{T}_h(\hat{\mathbf{r}}, z, s) = \int_0^\infty T(\hat{\mathbf{r}}, z, t)e^{-st}\,dt. \tag{21}$$

This form has the advantage of introducing the initial condition field explicitly into the equations. Note from (20) that the transient problem is converted into a nonhomogeneous problem due to Laplace transformation.

Being motivated by (12) and (19), we will consider a special class of initial conditions, i.e.,

$$T_{h0}(\hat{\mathbf{r}}, z) = u(\hat{\mathbf{r}}) + v(\hat{\mathbf{r}})e^{\zeta z} + w(\hat{\mathbf{r}})ze^{\zeta z}, \qquad \zeta \ge 0. \tag{22}$$

Bear in mind that (12) and (19) are special cases of (22) for which $\zeta = \delta$, etc. This special class of intial conditions includes the most interesting and probable case that the initial climate is in equilibrium, i.e., $T(\hat{\mathbf{r}}, z, t = 0) = 0$. One proceeds by assuming a solution

$$\tilde{T}_h(\hat{\mathbf{r}}, z, s) = f(\hat{\mathbf{r}}) + g(\hat{\mathbf{r}})e^{\zeta z} + h(\hat{\mathbf{r}})ze^{\zeta z} + \tilde{R}(\hat{\mathbf{r}}, z, s)e^{\lambda z}, \tag{23}$$

where $f(\hat{\mathbf{r}}) + g(\hat{\mathbf{r}})e^{\zeta z} + h(\hat{\mathbf{r}})ze^{\zeta z}$ is the particular solution of (20a) and $\tilde{R}(\hat{\mathbf{r}}, z, s)e^{\lambda z}$ is the homogeneous solution required to satisfy the boundary conditions. The position dependent coefficients satisfy partial differential equations in $\hat{\mathbf{r}}$. These equations may be formally solved and then the task is to invert the Laplace transforms. All but part of the last step can be performed analytically. The essential steps in the procedure are sketched in the appendix. The result of the computations just outlined is a numerical form for the homogeneous solution to both the step and the ramp forcings. In the next section we describe the findings.

4. Results and Discussion

First consider the solutions of the transient problem for ramp forcing ($F = \gamma t H(t)$). Figure 2 shows the vertical structures of $-T_{p0}$ in (19) at (0°N, 180°W) for $w = 4$ m yr^{-1}, $k = 4000$ m^2 yr^{-1}; $w = 4$, $k = 3000$; and for $w = 3$, $k = 4000$, respectively. Note that the values of w and k used in (8) are in line with those generally accepted by modelers of the deep ocean circulations [e.g., *Turner*, 1981; *Broecker*, 1981]. Aside from the linear trend in time, these figures represent the particular solutions of (9) for $F = \gamma t$ (also see equation (15)). Specifically, they are the temporal lags of the response to the radiative forcing. They are also the initial conditions for the homogeneous problem.

An interesting feature of these solutions is the heat accumulation near the permanent thermocline (the depth of which is defined to be $1/\delta = k/w$). An interplay of the upwelling and vertical diffusion traps a significant portion of the incoming energy near the permanent thermocline in the steady warming solution. The amount of energy trapped near the permanent thermocline may well be tied to the depth of the thermocline, which essentially determines the effective heat capacity. The larger the effective heat capacity is, the more the energy trapping is. As the upwelling speed w increases, energy trapping is decreased because the supply of cold water from below compensates the addition

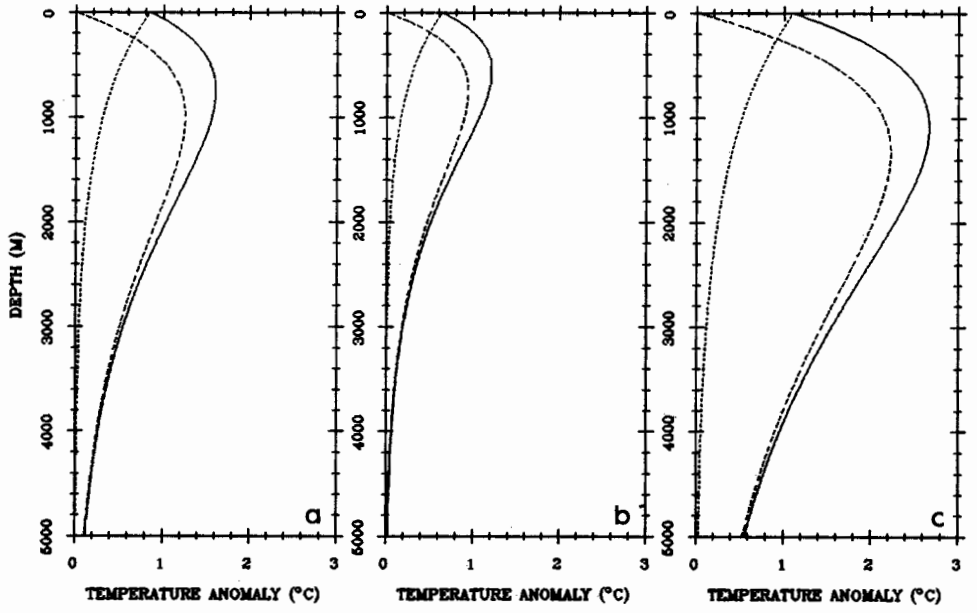

Fig. 2. Vertical structure of the initial condition, $-T_{p0}$, of the homogeneous problem at (0°N, 180°W) (*a*) for $w = 4$ m yr^{-1}, $k = 4000$ m^2 yr^{-1}; (*b*) for $w = 4$ m yr^{-1}, $k = 3000$ m^2 yr^{-1}; and (*c*) for $w = 3$ m yr^{-1}, $k = 4000$ m^2 yr^{-1}. Dotted lines are $\alpha\tau(\hat{\mathbf{r}})e^{\delta z}$, dashed lines are $\alpha(z/w)e^{\delta z}$, and the solid lines are the sum of the two. Aside from the response linear in time, the solid line essentially is a particular solution for $F(t) = \gamma t$.

of heat from above through the bottom of the mixed layer thereby decreasing the depth of the permanent thermocline. For a given w, however, the larger the vertical diffusion coefficient k is, the more deeply heat from the mixed layer is transported, thereby increasing the depth of the permanent thermocline.

Figure 3*a* is the temporal lag function, $\tau(\hat{\mathbf{r}})$, that should be used in the particular or asymptotic solution as computed from (18) for $w = 4$ m yr^{-1} and $k = 4000$ m^2 yr^{-1}. As might be expected from the low heat capacity, the land mass temperature change leads steady increase over the ocean

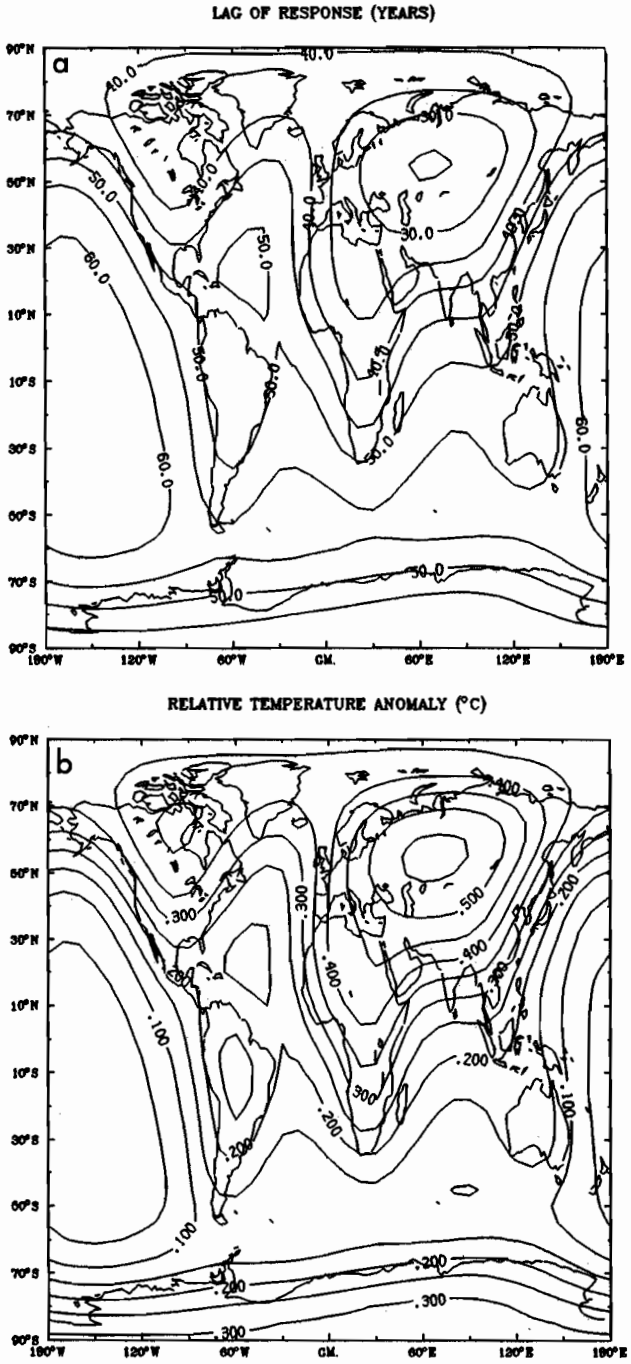

Fig. 3. Geography of (*a*) lag ($\tau(\hat{\mathbf{r}})$) in years and (*b*) the translated relative temperature anomaly in degree Celsius of the particular solution for $F(t) = \gamma t$. Here, $w = 4$ m yr^{-1} and $k = 4000$ m^2 yr^{-1}.

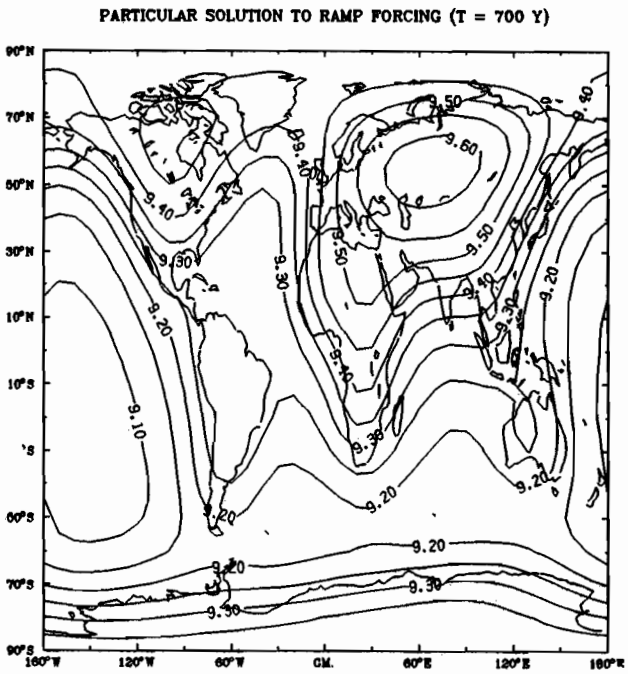

Fig. 4. Particular solution for $F(t) = \gamma t$ at $t = 700$ years. Here, $w = 4$ m yr^{-1} and $k = 4000$ m^2 yr^{-1}.

surface areas. As shown in Figure 3*b*, the temperature difference between central Asia and the central Pacific asymptotically approaches about 0.5°C for $\gamma = 0.03$ W m^{-2} yr^{-1} (equivalent to CO_2 doubling in 140 years). Observatio suggest a similar geographical dependence of different temperature rise between the land mass and the ocean [e.g., *Hansen and Lebedeff*, 1987]. It is misleading, however, to argue that the model response is correct solely on the basis of this comparison. Any rigorous comparison between the model and the observations requires examination of the homogeneous solution (transient response) as well as the particular solution (asymptotic response). Figure 4 shows the particular solution at time $t = 700$ years at the surface of the Earth.

Figure 5 shows the solutions (see (A2) in the appendix) of the homogeneous problem (10) over land (central Asia; 50°N, 90°E) and over the ocean (central Pacific; 0°N, 180°W) with $w = 4$ m yr^{-1} and $k = 4000$ m^2 yr^{-1}. Since we have no knowledge of the initial condition field (say, the temperature anomaly field in 1880 above or below the equilibrium state), we used $T_0(\hat{\mathbf{r}}, z) \equiv 0$ everywhere. Therefore, the initial condition for the homogeneous problem is

$$T_{h0} = -T_{p0} = \alpha(\tau(\hat{\mathbf{r}}) - z/w)e^{\delta z}. \tag{24}$$

The most prominent feature of the solution is its long decay time. While the temporal lag $\tau(\hat{\mathbf{r}})$ in Figure 3*a* is only about 60 years over the ocean, the actual temporal scale associated with the decay of the transient response is much longer, several hundred years, as is shown in Figure 5.

Scale analysis reveals that the temporal scales associated with the energy equation for the the ocean interior (7*a*) a the boundary condition (7*b*) are respectively

$$\tau_l = \left[\frac{1}{w\delta}, \frac{1}{k\delta^2}\right] = k/w^2 \approx 250 \text{ years};$$
$$\tau_s = \left[\frac{C(\hat{\mathbf{r}})}{wC^*(\hat{\mathbf{r}})}, \frac{C(\hat{\mathbf{r}})}{k\delta C^*(\hat{\mathbf{r}})}\right] = d_{\text{mix}}/w \approx 18 \text{ years}, \tag{25}$$

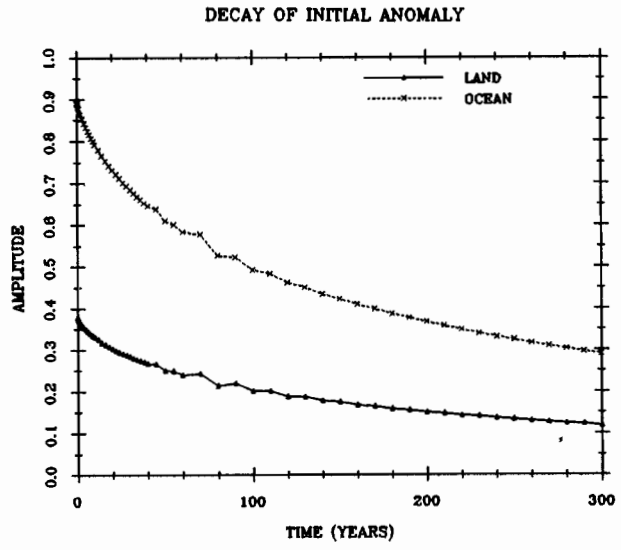

Fig. 5. Homogeneous solutions with the initial condition $T_{h0} = \alpha(\tau(\hat{\mathbf{r}}) - z/w)e^{\delta z}$. Solid line, typical land point (50°N, 90°E); dotted line, typical ocean point (0°N, 180°W). Here, $w = 4$ m yr^{-1} and $k = 4000$ m^2 yr^{-1}.

where $d_{\text{mix}} = 70$ m is the depth of the mixed layer. The latter represents the adjustment time scale in the mixed layer which is in thermal contact at its bottom with the deep ocean. If energy is added in the mixed layer (which is at the top of the deep ocean), the vertical structure of the temperature field changes such that the added thermal energy is to be transported downward into the deep ocean. This time scale is much shorter than the temporal lag shown in Figure 3*a*. The former represents the adjustment time scale in the deep ocean. Thermal energy added continuously into the deep ocean is redistributed such that the vertical diffusion and the upwelling balance each other. Therefore, the former is equivalently the time scale for the balance of the vertical diffusion and the upwelling. Scale analysis indicates that the deep ocean is responsible for the long decay time shown in Figure 5. A close examination of the structure of the solution in Figure 5 shows that there indeed exist two temporal scales. *Morantine and Watts* [1990] also reports the existence of two temporal scales. However, their definitions are somewhat different from (25).

For further examination of the dual temporal scales in the transient response, we divided the initial condition (24) into two parts:

$$T_{h0}^{(1)} = \alpha\tau(\hat{\mathbf{r}})e^{\delta z}, \quad (26)$$

$$T_{h0}^{(2)} = -\alpha(z/w)e^{\delta z}. \quad (27)$$

Solutions of the homogeneous problem with (26) and (27) indicate that there indeed are two temporal scales in the transient response as shown in Figure 6. The initial condition (26) is associated with the shorter temporal scale and is about 20 years over the ocean as in Figure 6*a*. The longer temporal scale is about 250 years as in Figure 6*b* and is associated with the forcing (equation (27)). The temporal scales derived in (25) match with the decay time scale in simulations with different values of w and k (not shown here).

Note from (12) that the initial condition for the instantaneous CO_2 doubling experiment is essentially (26) with $\tau(\hat{\mathbf{r}})$ replaced by unity. It is clear then from the above simulations that the time constant associated with the instantaneous doubling of CO_2 is about 20 years. This estimate is within the range of values estimated or inferred by a variety of climate/ocean models [e.g., *Schlesinger*, 1989; *Manabe et al.*, 1990; *Schlesinger and Jiang*, 1990].

Figure 7 shows the global temperature for the radiative forcing in the inset. The forcing represents the scenario A (business as usual) policy in controlling the use of fossil fuel [*Shine et al.*, 1990]. Between 1880 and 1980, the global temperature rise in our simple model is about 0.5°C. This is very consistent with the observed increase [*Hansen and Lebedeff*, 1987; *Jones et al.*, 1986]. It is worth noting that if the simulation is started in 1880 instead of a hundred years earlier, the increase in the last hundred years would be several tenths of a degree larger. The earlier starting time allows the long transient to decay significantly. (We are indebted to M. Hoffert for pointing out this subtle point to us.)

Figure 8 shows the complete transient solution of (7) (sum of particular solution (15) and homogeneous solution (A2)) for the radiative forcing in Figure 7. Because of the small effective heat capacity, land heats up faster than the ocean surface as shown in the maps. In 1980, simulation shows that central Asia is about 0.12°C warmer than the central

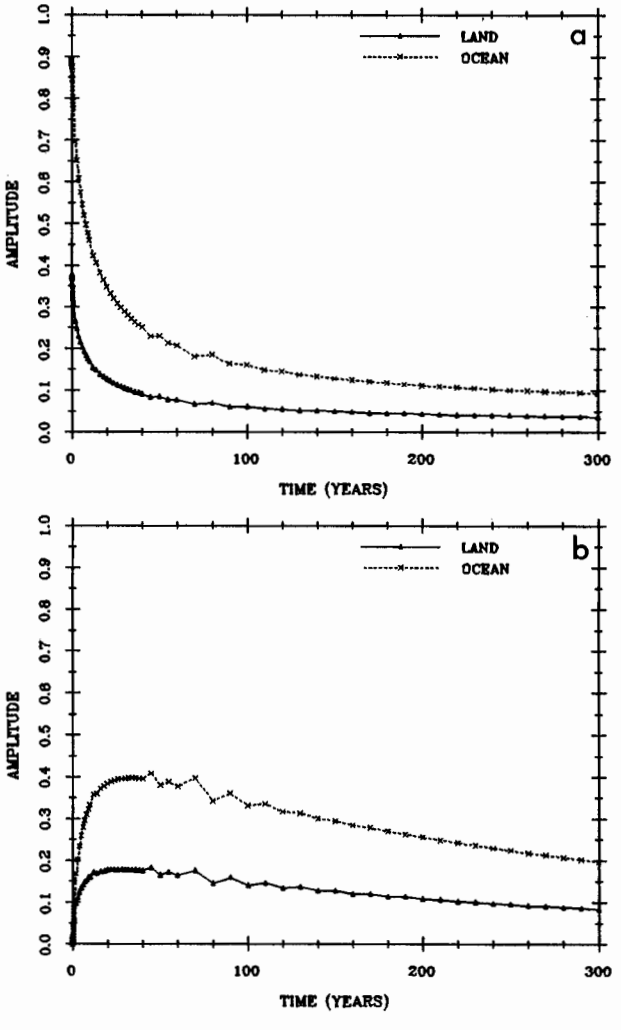

Fig. 6. Homogeneous solutions with the initial condition (*a*) $T_{h0} = \alpha\tau(\hat{\mathbf{r}})e^{\delta z}$, and (*b*) $T_{h0} = -\alpha(z/w)e^{\delta z}$. Solid line, typical land point (50°N, 90°E); dotted line, typical ocean point (0°N, 180°W). Here, $w = 4$ m yr^{-1} and $k = 4000$ m^2 yr^{-1}.

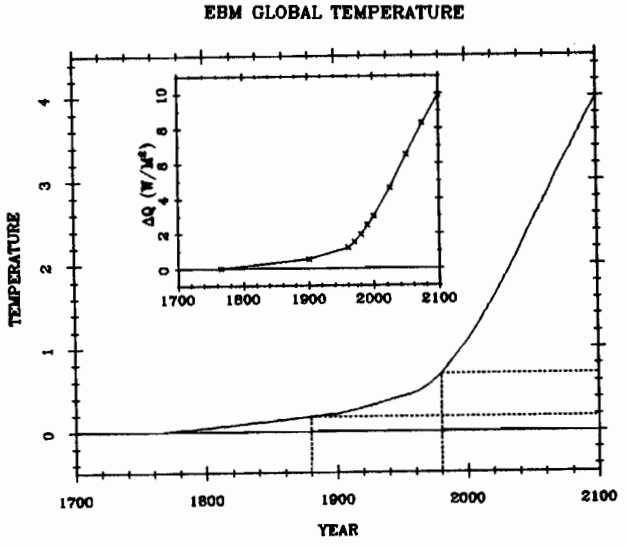

Fig. 7. Global temperature of EBM with deep upwelling-diffusion ocean for the scenario A (business as usual) policy. The radiative forcing is in the inset. Here, $w = 4$ m yr^{-1} and $k = 2000$ m^2 yr^{-1}.

Pacific. As the heat capacity contrast between land and the ocean becomes larger, the land-sea temperature difference in the case of ramp forcing becomes larger. Equivalently, as $1/\delta$ (thermocline depth) increases, this difference becomes larger. This temperature contrast, although somewhat small, is consistent with the observational record [*Hansen and Lebedeff*, 1987] and may constitute a "signature" worth exploring further.

Earlier studies have presented arguments that coupling to the ocean's interior (processes of upwelling and vertical diffusion) is responsible for the actual warming being only a fraction of that which would have occurred in the absence of the deep ocean. The deep ocean indeed contributes to delaying the warming due to the lag in the asymptotic form. However, the long adjustment time actually increases the early response at the surface due to the time required to fill out the vertical thermal profile of the waters below. Returning to Figure 1*a* we note that solution c will lie higher at a given time after onset for longer adjustment times and fixed lag time.

Keeping as close as possible to the present framework, we list a few additional considerations which might improve the model: (1) The model does not include time-dependent natural variability of such internal parameters as w, the upwelling rate, as suggested by *Watts and Morantine* [1991]. (2) There may be additional influences in the radiation entering the system to be incorporated in the heat budget such as aerosol. Such a perturbation could be easily incorporated if its time dependency were known [*Wigley*, 1989]. (3) Other possibilities include the shortcomings of the model connected with its lack of horizontal dependence of w and k together with no horizontal transport in the deep ocean. Locally large values of vertical transport could be short-circuited into the deep ocean and then smeared around. This mechanism would allow a faster reconstruction of the profile near the thermocline and effectively shorten the adjustment time to the asymptotic straight line. Some evidence for this response can be found in recent simulations with coupled ocean-atmosphere models [*Cubasch et al.*, 1991; *Manabe et al.*, 1991].

5. SUMMARY AND CONCLUSION

We examined the Earth's transient response by using simple energy balance model with a deep diffusive-upwell ocean. The model has an explicit two-dimensional geography. Vertical diffusion and upwelling are horizontally and vertically uniform throughout the water column. A technique based upon the Laplace transformation has been used to convert the problem into an almost analytically solvable one.

Model results show that for both ramp and step forcings, the land surfaces heat up to a given temperature level earlier than the ocean surfaces because of their smaller effective heat capacity. With a realistic rate of CO_2 increase, central Asia is about 0.12°C warmer than the central Pacific in 1980. Such a signature of differential heating is consistent qualitatively with the compilation of observations by *Hansen and Lebedeff* [1987]. The land-sea differential is a possibly important fingerprint that suggests further study involving signal-to-noise analysis.

In our past century experiment with a realistic radiative forcing, the simulated global temperature increases about ~ 0.5°C in 1980 relative to 1880. This estimate is consistent with that suggested in the observational record [e.g., *Jones et al.*, 1986; *Hansen and Lebedeff*, 1987]. We note that it was necessary to start the simulation 200 years before present to achieve the result. This permitted the slow transient to decay, significantly reducing the warming during the last hundred years.

It is usually argued that coupling to the deep ocean will delay the warming to a given value at a given time after t[1] onset of forcing. Such an intuitively appealing argumen based upon the analogy with a slab ocean. In the case o a just slightly more complex ocean the sequence of events is much more subtle due to the existence of several time constants instead of a single one.

As our analysis shows, there is a position-dependent lag of the asymptotic solution behind the imaginary instantaneously responding solution. In the case of ramp forcing, our complete model solutions suggest that this lag is a few decades. A much longer time scale enters in the transient adjustment to this asymptotic form. In order to fully adjust to the asymptotically linear curve, the surface may be warmer earlier than the water in the neighborhood of the thermocline while the latter adjusts to its asymptotic profile, which differs appreciably from the profile in static steady state equilibrium (local difference proportional to $(z/w)\exp(-wz/k)$). For the generally accepted model parameters we employed, this restructuring of the permanent thermocline for the ramp steady state takes several hundred years.

It is interesting that the restructuring of the deeper portions of the profile near the permanent thermocline is not as severe in the case of step forcing (local difference proportional only to $\exp(-wz/k)$). For this reason we find that an instantaneous doubling of CO_2 requires only a few decades for adjustment to its asymptotic constant value. As is already recognized, it is not a good idea to accept the single time found in step increase experiments to infer the adjv ment times for other forcing scenarios.

In summary, we list a few specific consequences of the existence of two temporal scales: (1) As was noted by *Thompson and Schneider* [1982], climate response to forcing linearly increasing in time is different from that due to instant CO_2 doubling. The former forcing induces a response with a

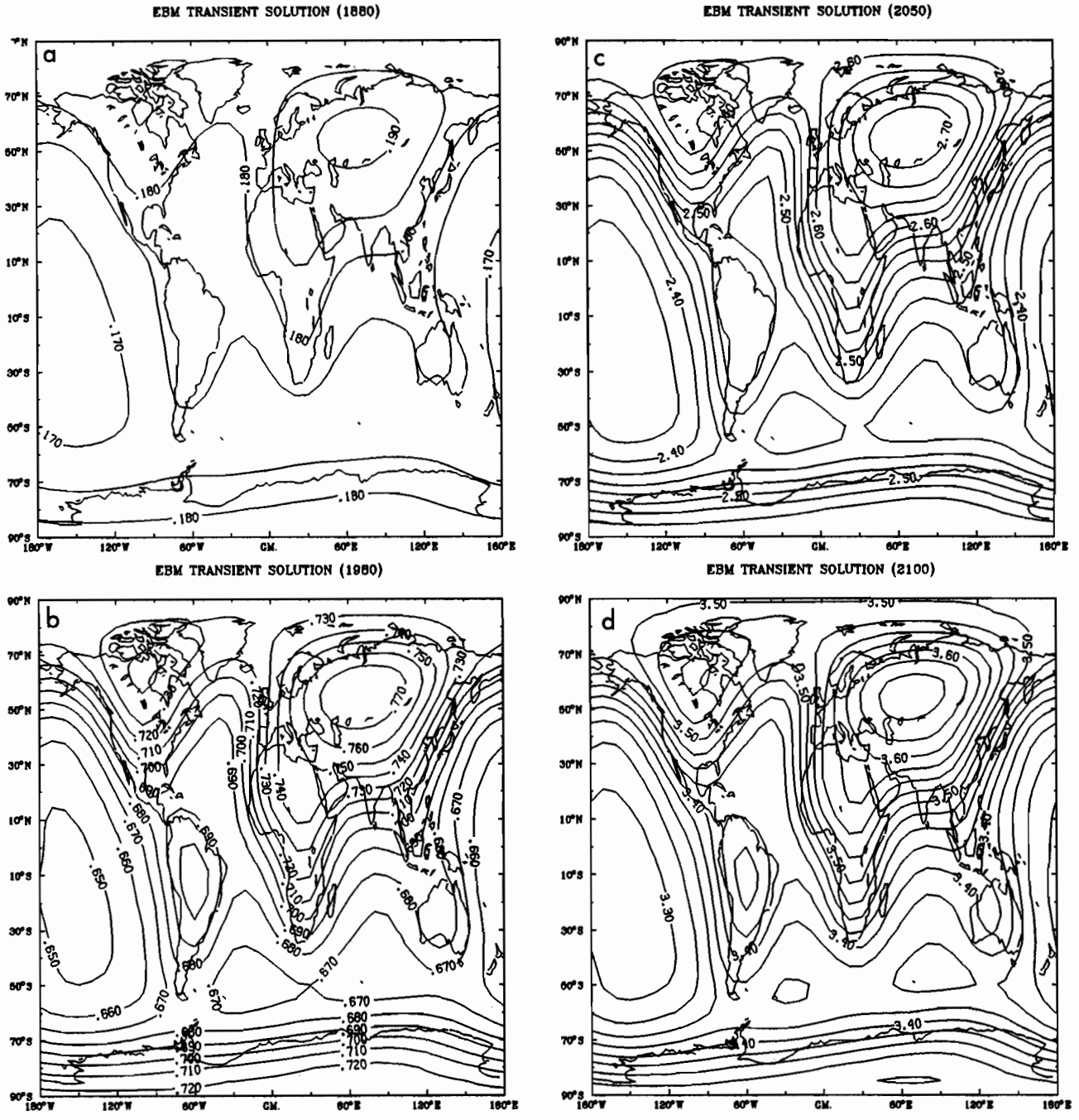

Fig. 8. Transient response of EBM with deep upwelling-diffusion ocean for the scenario A (business as usual) policy: (a) year 1880, (b) year 1980, (c) year 2050, and (d) year 2100. Here, $w = 4$ m yr^{-1} and $k = 2000$ m^2 yr^{-1}.

very long time scale (several hundred years) while the latter is very short (several decades). (2) Because of the sluggishness of the deep-ocean processes, the model ocean initially responds to ramp forcing similarly to a slab ocean response. At the onset, the incoming energy excess is mainly used to heat up the top of the ocean. Therefore, the ocean surface temperature increases rather rapidly and keeps up with the greenhouse gas forcing closely. Unlike the slab ocean, however, it takes several hundred years for model ocean to reach its asymptotic profile. (3) While there is no way of knowing exactly what the initial condition field was at the onset of greenhouse gas forcing (say, temperature anomaly in 1780 from the true equilibrium state), observational evidence seems to suggest that there was a warm anomaly. If the vertical structure of such natural fluctuation is $e^{\delta z}$, it will decay rapidly. As was shown earlier, the transient signal of this anomaly is almost zero after 100 years. Thus an accurate knowledge of the initial condition and its vertical structure is extremely important in addressing the global temperature rise during 1880–1980.

Before ending this discussion we wish to remind the reader that we are not advocating the simple ocean model used here as an ultimate tool to use in greenhouse gas warming scenarios. In fact, we believe that the model is too simple. The adjustment times are likely to be shorter. We suspect that at least part of the problem lies in our assumption of

horizontally uniform values of the vertical transport parameters and the lack of horizontal transport in the lower ocean. Combining nonuniform transport and horizontal transport is likely to increase thermal communication between layers and speed up the adjustment process in the case of ramp forcing.

We feel the approach taken here is likely to prove useful in gaining a better understanding of the global warming problem. For example, we intend to use similar models to study noise-forced fluctuations of the temperature field similar the work conducted by *Kim and North* [1991] based u a mixed-layer-only model. Such studies shed light on the many signal-to-noise issues that are vital to completing the picture of climate change detectability and predictability.

APPENDIX

For a special class of initial conditions

$$T_{h0}(\hat{\mathbf{r}}, z) = u(\hat{\mathbf{r}}) + v(\hat{\mathbf{r}})e^{\zeta z} + w(\hat{\mathbf{r}})ze^{\zeta z}, \qquad \zeta \geq 0, \quad \text{(A1)}$$

one finds a solution of (20) in the form

$$\widetilde{T}_h(\hat{\mathbf{r}}, z, s) = f(\hat{\mathbf{r}}) + g(\hat{\mathbf{r}})e^{\zeta z} + h(\hat{\mathbf{r}})ze^{\zeta z} + \widetilde{R}(\hat{\mathbf{r}}, z, s)e^{\lambda z}, \quad \text{(A2)}$$

where $f(\hat{\mathbf{r}}) + g(\hat{\mathbf{r}})e^{\zeta z} + h(\hat{\mathbf{r}})ze^{\zeta z}$ is the particular solution (satisfying the nonhomogeneous problem with T_{h0} given by (A1)) while $\widetilde{R}(\hat{\mathbf{r}})e^{\lambda z}$ is the homogeneous solution (satisfying the Sturm-Liouville problem with $T_{h0} = 0$). Here the eigenvalue λ is defined by

$$\begin{aligned} \lambda &= \frac{w + \sqrt{w^2 + 4ks}}{2k} = \frac{\delta}{2} + \mu; \\ \delta &= w/k; \\ \mu &= \sqrt{s/k + \delta^2/4}. \end{aligned}$$

It readily follows from (20a) that

$$\begin{aligned} f(\hat{\mathbf{r}}) &= u(\hat{\mathbf{r}})/s; \\ g(\hat{\mathbf{r}}) &= \frac{-v(\hat{\mathbf{r}})}{k\zeta^2 - w\zeta - s} + \frac{(2k\zeta - w)w(\hat{\mathbf{r}})}{(k\zeta^2 - w\zeta - s)^2}; \\ h(\hat{\mathbf{r}}) &= \frac{-w(\hat{\mathbf{r}})}{k\zeta^2 - w\zeta - s}. \end{aligned}$$

Therefore,

$$\begin{aligned} \widetilde{T}_h(\hat{\mathbf{r}}, z, s) = \widetilde{R}(\hat{\mathbf{r}}, z, s)e^{\lambda z} + \frac{u(\hat{\mathbf{r}})}{s} - \frac{w(\hat{\mathbf{r}})}{k\zeta^2 - w\zeta - s}ze^{\zeta z} \\ - \frac{v(\hat{\mathbf{r}})}{k\zeta^2 - w\zeta - s}e^{\zeta z} + \frac{(2k\zeta - w)w(\hat{\mathbf{r}})}{(k\zeta^2 - w\zeta - s)^2}e^{\zeta z}. \end{aligned}$$

Now, from the boundary condition

$$\begin{aligned} &\Big[C(\hat{\mathbf{r}}) + \frac{1}{s}\big\{B - \nabla\cdot\big(D(x)\nabla\big) - wC^*(\hat{\mathbf{r}})\big\} + \frac{\lambda}{s}kC^*(\hat{\mathbf{r}})\Big]\widetilde{R}(\hat{\mathbf{r}}, z, s)e^{\lambda z} \\ &= -C(\hat{\mathbf{r}})\Big\{-\frac{v(\hat{\mathbf{r}})}{s} - \frac{v(\hat{\mathbf{r}})}{k\zeta^2 - w\zeta - s} + \frac{(2k\zeta - w)w(\hat{\mathbf{r}})}{(k\zeta^2 - w\zeta - s)^2}\Big\}e^{\lambda z} \\ &-\Big\{B - \nabla\big(D(x)\nabla\big) - wC^*(\hat{\mathbf{r}})\Big\}\Big[\frac{u(\hat{\mathbf{r}})}{s^2} - \frac{v(\hat{\mathbf{r}})}{s(k\zeta^2 - w\zeta - s)} + \frac{(2k\zeta - w)w(\hat{\mathbf{r}})}{s(k\zeta^2 - w\zeta - s)^2}\Big]e^{\lambda z} \\ &-kC^*(\hat{\mathbf{r}})\Big[-\frac{\zeta v(\hat{\mathbf{r}})}{s(k\zeta^2 - w\zeta - s)} - \frac{w(\hat{\mathbf{r}})}{s(k\zeta^2 - w\zeta - s)} + \frac{\zeta(2k\zeta - w)w(\hat{\mathbf{r}})}{s(k\zeta^2 - w\zeta - s)^2}\Big]e^{\lambda z}. \end{aligned} \quad \text{(A3)}$$

Taking the inverse Laplace transformation of (A3) [see *Abramowitz and Stegun*, 1971], we obtain

$$\begin{aligned} &C(\hat{\mathbf{r}})R(\hat{\mathbf{r}}, z, t) + \Big\{B - \nabla\cdot\big(D(x)\nabla\big) - \frac{w}{2}C^*(\hat{\mathbf{r}})\Big\}\int_0^t R(\hat{\mathbf{r}}, z, \tau)\,d\tau \\ &+kC^*(\hat{\mathbf{r}})\int_0^t R(\hat{\mathbf{r}}, z, \tau)e^{-(\delta^2 k/4)(t-\tau)}\Big\{\frac{1}{\sqrt{\pi k(t-\tau)}} + \frac{\delta}{2}e^{(\delta^2 k/4)(t-\tau)}\mathrm{erf}\big(\sqrt{(\delta^2 k/4)(t-\tau)}\big)\Big\}\,d\tau \\ &= C(\hat{\mathbf{r}})f_1(\hat{\mathbf{r}}, z, t) - \big\{B - \nabla\cdot\big(D(x)\nabla\big) - wC^*(\hat{\mathbf{r}})\big\}f_2(\hat{\mathbf{r}}, z, t) - kC^*(\hat{\mathbf{r}})f_3(\hat{\mathbf{r}}, z, t), \end{aligned} \quad \text{(A4)}$$

where

$$
\begin{aligned}
(\hat{\mathbf{r}}, z, t) &= \frac{v(\hat{\mathbf{r}})}{2}\left\{e^{-\delta z/2}\operatorname{erfc}\left(-\frac{\delta}{2}-\frac{z}{2\sqrt{kt}}\right)+e^{\delta z/2}\operatorname{erfc}\left(\frac{\delta}{2}-\frac{z}{2\sqrt{kt}}\right)\right\}\\
&-\frac{v(\hat{\mathbf{r}})}{2}\left\{e^{-(\zeta-\delta/2)z}e^{\zeta(\zeta-\delta)kt}\operatorname{erfc}\left(-(\zeta-\delta/2)\sqrt{kt}-\frac{z}{2\sqrt{kt}}\right)+e^{(\zeta-\delta/2)z}e^{\zeta(\zeta-\delta)kt}\operatorname{erfc}\left((\zeta-\delta/2)\sqrt{kt}-\frac{z}{2\sqrt{kt}}\right)\right\}\\
&-\frac{w(\hat{\mathbf{r}})}{2}(2k\zeta-w)\int_0^t e^{-(\zeta-\delta/2)z}e^{\zeta(\zeta-\delta)k\tau}\operatorname{erfc}\left(-(\zeta-\delta/2)\sqrt{k\tau}-\frac{z}{2\sqrt{k\tau}}\right)\\
&\quad+e^{(\zeta-\delta/2)z}e^{\zeta(\zeta-\delta)k\tau}\operatorname{erfc}\left((\zeta-\delta/2)\sqrt{k\tau}-\frac{z}{2\sqrt{k\tau}}\right)d\tau,
\end{aligned}
$$

$$
\begin{aligned}
f_2(\hat{\mathbf{r}}, z, t) &= \frac{u(\hat{\mathbf{r}})}{2}\int_0^t e^{-\delta z/2}\operatorname{erfc}\left(-\frac{\delta}{2}\sqrt{k\tau}-\frac{z}{2\sqrt{k\tau}}\right)+e^{\delta z/2}\operatorname{erfc}\left(\frac{\delta}{2}\sqrt{k\tau}-\frac{z}{2\sqrt{k\tau}}\right)d\tau\\
&+\frac{v(\hat{\mathbf{r}})}{2}\int_0^t e^{-(\zeta-\delta/2)z}e^{\zeta(\zeta-\delta)k\tau}\operatorname{erfc}\left(-(\zeta-\delta/2)\sqrt{k\tau}-\frac{z}{2\sqrt{k\tau}}\right)\\
&\quad+e^{(\zeta-\delta/2)z}e^{\zeta(\zeta-\delta)k\tau}\operatorname{erfc}\left((\zeta-\delta/2)\sqrt{k\tau}-\frac{z}{2\sqrt{k\tau}}\right)d\tau\\
&+\frac{w(\hat{\mathbf{r}})}{2}\frac{2k\zeta-w}{\zeta(\delta-\zeta)}I_{\{\zeta\neq\delta\}}\int_0^t e^{-(\zeta-\delta/2)z}\left\{e^{\zeta(\zeta-\delta)k\tau}-e^{\zeta(\zeta-\delta)kt}\right\}\operatorname{erfc}\left(-(\zeta-\delta/2)\sqrt{k\tau}-\frac{z}{2\sqrt{k\tau}}\right)\\
&\quad+e^{(\zeta-\delta/2)z}\left\{e^{\zeta(\zeta-\delta)k\tau}-e^{\zeta(\zeta-\delta)kt}\right\}\operatorname{erfc}\left((\zeta-\delta/2)\sqrt{k\tau}-\frac{z}{2\sqrt{k\tau}}\right)d\tau\\
&+\frac{w(\hat{\mathbf{r}})}{2}(2k\zeta-w)I_{\{\zeta=\delta\}}\int_0^t(t-\tau)\left\{e^{-\delta z/2}\operatorname{erfc}\left(-\frac{\delta}{2}\sqrt{k\tau}-\frac{z}{2\sqrt{k\tau}}\right)+e^{\delta z/2}\operatorname{erfc}\left(\frac{\delta}{2}\sqrt{k\tau}-\frac{z}{2\sqrt{k\tau}}\right)\right\}d\tau,
\end{aligned}
$$

$$
\begin{aligned}
f_3(\hat{\mathbf{r}}, z, t) &= \frac{\zeta v(\hat{\mathbf{r}})+w(\hat{\mathbf{r}})}{2}\\
&\times\int_0^t e^{-(\zeta-\delta/2)z}e^{\zeta(\zeta-\delta)k\tau}\operatorname{erfc}\left(-(\zeta-\delta/2)\sqrt{k\tau}-\frac{z}{2\sqrt{k\tau}}\right)+e^{(\zeta-\delta/2)z}e^{\zeta(\zeta-\delta)k\tau}\operatorname{erfc}\left((\zeta-\delta/2)\sqrt{k\tau}-\frac{z}{2\sqrt{k\tau}}\right)d\tau\\
&+\frac{w(\hat{\mathbf{r}})}{2}\frac{2k\zeta-w}{\delta-\zeta}I_{\{\zeta\neq\delta\}}\int_0^t e^{-(\zeta-\delta/2)z}\left\{e^{\zeta(\zeta-\delta)k\tau}-e^{\zeta(\zeta-\delta)kt}\right\}\operatorname{erfc}\left(-(\zeta-\delta/2)\sqrt{k\tau}-\frac{z}{2\sqrt{k\tau}}\right)\\
&\quad+e^{(\zeta-\delta/2)z}\left\{e^{\zeta(\zeta-\delta)k\tau}-e^{\zeta(\zeta-\delta)kt}\right\}\operatorname{erfc}\left((\zeta-\delta/2)\sqrt{k\tau}-\frac{z}{2\sqrt{k\tau}}\right)d\tau\\
&+\frac{w(\hat{\mathbf{r}})}{2}\zeta(2k\zeta-w)I_{\{\zeta=\delta\}}\int_0^t(t-\tau)\left\{e^{-\delta z/2}\operatorname{erfc}\left(-\frac{\delta}{2}\sqrt{k\tau}-\frac{z}{2\sqrt{k\tau}}\right)+e^{\delta z/2}\operatorname{erfc}\left(\frac{\delta}{2}\sqrt{k\tau}-\frac{z}{2\sqrt{k\tau}}\right)\right\}d\tau,
\end{aligned}
$$

and

$$
I_{\{\text{expression}\}}=\begin{cases}1, & \text{if expression is true;}\\ 0, & \text{otherwise.}\end{cases}
$$

Therefore,

$$
\begin{aligned}
T(\hat{\mathbf{r}}, z, t) &= u(\hat{\mathbf{r}})+\left\{v(\hat{\mathbf{r}})+zw(\hat{\mathbf{r}})\right\}e^{\zeta z}e^{\zeta(\zeta-\delta)kt}\\
&\quad+(2k\zeta-w)w(\hat{\mathbf{r}})te^{\zeta z}e^{\zeta(\zeta-\delta)kt}+R(\hat{\mathbf{r}}, z, t).
\end{aligned}
$$

For computational reasons, we rewrite (A4) as follows:

$$
\begin{aligned}
&C(\hat{\mathbf{r}})R(\hat{\mathbf{r}}, z, t_n)+\left\{B-\nabla\cdot\left(D(x)\nabla\right)-\frac{w}{2}C^*(\hat{\mathbf{r}})\right\}\int_{t_{n-1}}^{t_n}R(\hat{\mathbf{r}}, z, \tau)\,d\tau\\
&+\frac{w}{2}C^*(\hat{\mathbf{r}})\int_{t_{n-1}}^{t_n}R(\hat{\mathbf{r}}, z, \tau)\operatorname{erf}\left(\sqrt{(\delta^2k/4)(t_n-\tau)}\right)d\tau\\
&+kC^*(\hat{\mathbf{r}})\int_{t_{n-1}}^{t_n}R(\hat{\mathbf{r}}, z, \tau)\frac{1}{\sqrt{\pi k(t_n-\tau)}}e^{-(\delta^2k/4)(t_n-\tau)}\,d\tau\\
&=-\left\{B-\nabla\cdot\left(D(x)\nabla\right)-\frac{w}{2}C^*(\hat{\mathbf{r}})\right\}\int_0^{t_{n-1}}R(\hat{\mathbf{r}}, z, \tau)\,d\tau
\end{aligned}
$$

$$-\frac{w}{2}C^*(\hat{\mathbf{r}})\int_0^{t_{n-1}} R(\hat{\mathbf{r}},z,\tau)\operatorname{erf}\left(\sqrt{(\delta^2 k/4)(t_n-\tau)}\right)d\tau$$
$$-kC^*(\hat{\mathbf{r}})\int_0^{t_{n-1}} R(\hat{\mathbf{r}},z,\tau)\frac{1}{\sqrt{\pi k(t_n-\tau)}}e^{-(\delta^2 k/4)(t_n-\tau)}\,d\tau$$
$$+C(\hat{\mathbf{r}})f_1(\hat{\mathbf{r}},z,t_n)-\left\{B-\nabla\cdot\left(D(x)\nabla\right)-wC^*(\hat{\mathbf{r}})\right\}f_2(\hat{\mathbf{r}},z,t_n)-kC^*(\hat{\mathbf{r}})f_3(\hat{\mathbf{r}},z,t_n), \tag{A5}$$

where t_n is the nth time step. Using the finite-difference method, it can be shown that

$$\int_{t_{n-1}}^{t_n} R(\hat{\mathbf{r}},z,\tau)\,d\tau=\frac{\Delta t_n}{2}(R_n+R_{n-1});$$

$$\int_{t_{n-1}}^{t_n} R(\hat{\mathbf{r}},z,\tau)\operatorname{erf}\left(\sqrt{(\delta^2 k/4)(t_n-\tau)}\right)d\tau=\frac{\Delta t_n}{2}\operatorname{erf}\left(\sqrt{(\delta^2 k/4)\Delta t_n}\right)R_{n-1};$$

$$\begin{aligned}
&\int_{t_{n-1}}^{t_n} R(\hat{\mathbf{r}},z,\tau)\frac{1}{\sqrt{\pi k(t_n-\tau)}}e^{-(\delta^2 k/4)(t_n-\tau)}\,d\tau\\
&\quad=-\frac{2\sqrt{t_n-\tau}}{\sqrt{\pi k}}e^{-(\delta^2 k/4)(t_n-\tau)}R(\hat{\mathbf{r}},z,\tau)\Big|_{\tau=t_{n-1}}^{t_n}\\
&\qquad+\int_{t_{n-1}}^{t_n}\frac{2\sqrt{t_n-\tau}}{\sqrt{\pi k}}e^{-(\delta^2 k/4)(t_n-\tau)}\left\{(\delta^2 k/4)R(\hat{\mathbf{r}},z,\tau)+\frac{dR(\hat{\mathbf{r}},z,\tau)}{d\tau}\right\}d\tau\\
&\quad\doteq\frac{2\sqrt{\Delta t_n}}{\sqrt{\pi k}}e^{-(\delta^2 k/4)\Delta t_n}R_{n-1}+\frac{\Delta t_n}{2}\frac{2\sqrt{\Delta t_n}}{\sqrt{\pi k}}e^{-(\delta^2 k/4)\Delta t_n}\left[(\delta^2 k/4)R_{n-1}+\frac{R_n-R_{n-1}}{\Delta t_n}\right]\\
&\quad=\frac{\sqrt{\Delta t_n}}{\sqrt{\pi k}}e^{-(\delta^2 k/4)\Delta t_n}\left[\left\{1+(\delta^2 k/4)\Delta t_n\right\}R_{n-1}+R_n\right],
\end{aligned}$$

where $R_n=R(\hat{\mathbf{r}},z,t_n)$ and $\Delta t_n=t_n-t_{n-1}$. Therefore a finite-difference analog of (A5) in time is written as

$$UR_n=VR_{n-1}+f, \tag{A6}$$

where the operators U and V are respectively

$$U=C(\hat{\mathbf{r}})+\frac{\Delta t_n}{2}\left\{B-\nabla\cdot\left(D(x)\nabla\right)\right\}+\left[\frac{\sqrt{k\Delta t_n}}{\sqrt{\pi}}e^{-(\delta^2 k/4)\Delta t_n}-\frac{\Delta t_n}{4}w\right]C^*(\hat{\mathbf{r}})$$

$$\begin{aligned}
V=&-\frac{\Delta t_n}{2}\left\{B-\nabla\cdot\left(D(x)\nabla\right)\right\}-\left[\frac{\sqrt{k\Delta t_n}}{\sqrt{\pi}}e^{-(\delta^2 k/4)\Delta t_n}\left\{1+\delta^2 k/4)\Delta t_n\right\}\right.\\
&\left.+\frac{\Delta t_n}{4}w\left\{\operatorname{erf}\left(\sqrt{(\delta^2 k/4)(t_n-\tau)}\right)-1\right\}\right]C^*(\hat{\mathbf{r}})
\end{aligned}$$

and

$$\begin{aligned}
f=&-\left\{B-\nabla\cdot\left(D(x)\nabla\right)\right\}\int_0^{t_{n-1}} R(\hat{\mathbf{r}},z,\tau)\,d\tau+\frac{w}{2}C^*(\hat{\mathbf{r}})\int_0^{t_{n-1}} R(\hat{\mathbf{r}},z,\tau)\,d\tau\\
&-\frac{w}{2}C^*(\hat{\mathbf{r}})\int_0^{t_{n-1}} R(\hat{\mathbf{r}},z,\tau)\operatorname{erf}\left(\sqrt{(\delta^2 k/4)(t_n-\tau)}\right)d\tau-kC^*(\hat{\mathbf{r}})\int_0^{t_{n-1}} R(\hat{\mathbf{r}},z,\tau)\frac{1}{\sqrt{\pi k(t_n-\tau)}}e^{-(\delta^2 k/4)(t_n-\tau)}\,d\tau\\
&+C(\hat{\mathbf{r}})f_1(\hat{\mathbf{r}},z,t_n)-\left\{B-\nabla\cdot\left(D(x)\nabla\right)-wC^*(\hat{\mathbf{r}})\right\}f_2(\hat{\mathbf{r}},z,t_n)-kC^*(\hat{\mathbf{r}})f_3(\hat{\mathbf{r}},z,t_n).
\end{aligned}$$

In terms of the spherical harmonic basis functions, (A6) is further rewritten as

$$M\underline{R}^n=N\underline{R}^{n-1}+\underline{f},$$

or equivalently,

$$M_{ij}R_j^n=N_{ij}R_j^{n-1}+f_i,$$

where $\underline{R}^n(z) = \{R^n_{lm}(z) | \ 0 \le l \le L; -l \le m \le l\}$ is the expansion coefficients of $R^n(\hat{\mathbf{r}}, z)$, i.e.,

$$R^n(\hat{\mathbf{r}}, z) = \sum_{l=0}^{L} \sum_{|m| \le l} R^n_{lm}(z) Y_l^m(\hat{\mathbf{r}}),$$

$$= \sum_i R^n_i(z) Y_i(\hat{\mathbf{r}}),$$

and

$$M_{ij} = \int \left(U Y_j(\hat{\mathbf{r}})\right) Y_i^*(\hat{\mathbf{r}})\, d\Omega,$$

$$N_{ij} = \int \left(V Y_j(\hat{\mathbf{r}})\right) Y_i^*(\hat{\mathbf{r}})\, d\Omega,$$

$$f_i = \int f Y_i^*(\hat{\mathbf{r}})\, d\Omega.$$

Here, $Y_l^m(\hat{\mathbf{r}})$ is the spherical harmonic function of order l and rank m, and L is the maximum expansion order of $R^n(\hat{\mathbf{r}}, z)$.

Acknowledgments. We thank the Department of Energy for its support of this work via a grant to Texas A&M University through its Quantitative Links Initiative and to Applied Research Corporation through CHAMMP (DE-FG05-91ER61221) and a subcontract with the Battelle Pacific Northwest Laboratories. The Department of Energy does not necessarily endorse any of the conclusions drawn in the paper. We also wish to thank Thomas Crowley, Martin Hoffert, Michael MacCracken, and Inez Fung for helpful discussions.

REFERENCES

Abramowitz, M., and I. A. Stegun, *Handbook of Mathematical Functions with Formulas, Graphs, and Mathematical Tables*, 1046 pp., Dover, New York, 1971.

Broecker, W. S., Geochemical tracers and ocean circulation, in *Evolution of Physical Oceanography*, edited by B. A. Warren and C. Wunsch, pp. 236–262, MIT Press, Cambridge, Mass., 1981.

Cubasch, U., K. Hasselmann, H. Höck, E. Maier-Reimer, U. Mikolajewicz, B. D. Santer, and R. Sausen, Time-dependent greenhouse warming computations with a coupled ocean-atmosphere model, *Rep. 67*, 18 pp., Max-Planck-Inst. für Meteorol., Hamburg, Germany, 1991.

Hansen, J., and S. Lebedeff, Global trends of measured surface air temperature, *J. Geophys. Res.*, *92*, 13,345–13,372, 1987.

Hoffert, M. I., and B. F. Flannery, Model projections of the time-dependent response to increasing carbon dioxide, in Projecting the Climate Effects of Increasing Carbon Dioxide, *Rep. DOE/ER-0237*, edited by M. C. MacCracken and F. M. Luther, pp. 149–190, U. S. Dep. of Energy, Washington, D.C., 1985.

Hoffert, M. I., A. J. Callegari, and C.-T. Hsieh, The role of deep sea heat storage in the secular response to climatic forcing, *J. Geophys. Res.*, *85*, 6667–6679, 1980.

Hyde, W., T. J. Crowley, K.-Y. Kim, and G. R. North, Comparison of GCM and energy balance model simulations of seasonal temperature changes over the past 18000 years, *J. Clim.*, *2*, 864–887, 1989.

Hyde, W., K.-Y. Kim, T. J. Crowley, and G. R. North, On the relationship between polar continentality and climate: Studies with a nonlinear seasonal energy balance model, *J. Geophys. Res.*, *95*, 18,653–18,668, 1990.

Jones, P. D., T. M. L. Wigley, and P. B. Wright, Global temperature variations between 1861 and 1984, *Nature*, *322*, 430–434, 1986.

Kim, K.-Y., and G. R. North, Surface temperature fluctuations in a stochastic climate model, *J. Geophys. Res.*, *96*, 18,573–18,580, 1991.

Lebedeff, S. A., Analytical solution of the box diffusion model for a global ocean, *J. Geophys. Res.*, *93*, 14,243–14,255, 1988.

Leung, L., and G. R. North, Atmospheric variability on a zonally symmetric all land planet, *J. Clim.*, *4*, 753–765, 1992.

Manabe, S., K. Bryan, and M. J. Spelman, Transient response of a global ocean-atmosphere model to a doubling of atmospheric carbon dioxide, *J. Phys. Oceanogr.*, *20*, 722–749, 1990.

Manabe, S., R. J. Stouffer, M. J. Spelman, and K. Bryan, Transient responses of a coupled ocean-atmosphere model to gradual changes of atmospheric CO_2, I, Annual mean response, *J. Clim.*, *4*, 785–818, 1991.

Morantine, M., and R. G. Watts, Upwelling diffusion climate model: Analytical solutions for radiative and upwelling forcing, *J. Geophys. Res.*, *95*, 7563–7571, 1990.

Munk, W. H., Abyssal recipes, *Deep Sea Res.*, *13*, 707–730, 1966.

North, G. R., J. Mengel, and D. Short, Simple energy balance model resolving the seasons and the continents: Application to the astronomical theory of the ice ages, *J. Geophys. Res.*, *88*, 6576–6586, 1983*a*.

North, G. R., J. Mengel, and D. Short, On the transient response patterns of climate to time dependent concentrations of atmospheric CO_2, in *Climate Processes and Climate Sensitivity*, *Geophys. Monogr. Ser.*, Vol. 29, edit by J. E. Hansen and T. Takahashi, pp. 164–170, AGU, Washington, D.C., 1983*b*.

North, G. R., K. Yip, L. Leung, and R. Chervin, Forced and free variations of the surface temperature field in a general circulation model, *J. Clim.*, *5*, 227–239, 1992.

Overstreet, R., and M. Rattray, On the roles of vertical velocity and eddy conductivity in maintaining a thermocline, *J. Mar. Res.*, *27*(2), 172–190, 1969.

Schlesinger, M. E., Model projections of the climate changes induced by increased atmospheric CO_2, in *Climate and the Geo-Sciences; A Challenge for Science and Society in the 21st Century*, edited by A. Berger, S. Schneider, and J. C. Duplessy, pp. 375–415, Kluwer Academic, Boston, Mass., 1989.

Schlesinger, M. E., and X. Jiang, Simple model representation of atmosphere-ocean GCMs and estimation of the time scale of CO_2-induced climate change, *J. Clim.*, *3*, 1297–1315, 1990.

Schlesinger, M. E., and X. Jiang, Revised projection of future greenhouse warming, *Nature*, *350*, 219–221, 1991.

Schlesinger, M. E., W. L. Gates, and Y.-J. Han, The role of the ocean in CO_2-induced climate warming; Preliminary results from the OSU compled atmosphere-ocean GCM, in *Coupled Ocean-Atmosphere Models*, edited by J. C. J. Nihoul, pp. 447–478, Elsevier, New York, 1985.

Shine, K. P., R. G. Derwent, D. J. Wuebbles, and J.-J. Morcrette, Radiative forcing of climate, in *Climate Change, The IPCC Scientific Assessment*, edited by J. T. Houghton, G. J. Jenkins and J. J. Ephraums, pp. 41–68, Cambridge University Press, New York, 1990.

Thompson, S. L., and S. H. Schneider, Carbon dioxide and climate; The importance of realistic geography in estimating the transient temperature response, *Science*, *217*, 1031–1033, 1982.

Turner, J. S., Small-scale mixing processes, in *Evolution of Physical Oceanography*, edited by B. A. Warren and C. Wunsch, pp. 236–262, MIT Press, Cambridge, Mass., 1981.

Washington, W. M., and G. A. Meehl, Climate sensitivity due to increased CO_2: Experiments with a coupled atmosphere and ocean general circulation model, *Clim. Dyn.*, *4*, 1–38, 1989.

Watts, R. G., and M. Morantine, Rapid climatic change and the deep ocean, *Clim. Change*, *16*, 83–97, 1990.

Watts, R. G., and M. Morantine, Is the greenhouse gas-climate signal hiding in the deep ocean?, *Clim. Change*, *18*, iii–vi, 1991.

Wigley, T. M. L., The effect of model structure on projections of greenhouse-gas-induced climatic change, *Geophys. Res. Letts.*, *14*, 1135–1138, 1987.

Wigley, T. M. L., Possible climate change due to SO_2-derived cloud condensation nuclei, *Nature*, *339*, 365–367, 1989.

Wigley, T. M. L., and S. C. B. Raper, Natural variability of the climate system and detection of the greenhouse effect, *Nature*, *344*, 324–327, 1990.

J. Huang and G. R. North, Climate System Research Program, Department of Meteorology, Texas A&M University, College Station, TX 77843.

K.-Y. Kim, Applied Research Corporation, 305 Arguello Drive, College Station, TX 77840.

(Received August 26, 1991;
revised February 28, 1992;
accepted March 5, 1992.)